JOURNAL OF NEUROPHYSIOLOGY
Vol. 73, No. 3, March 1995. *Printed in U.S.A.*

Hysteresis Reduction in Proprioception Using Presynaptic Shunting Inhibition

NICHOLAS G. HATSOPOULOS, MALCOLM BURROWS, AND GILLES LAURENT
Computation and Neural Systems Program, Division of Biology, 139–74, California Institute of Technology, Pasadena, California 91125

SUMMARY AND CONCLUSIONS

1. The tonic responses of angular-position–sensitive afferents in the metathoracic chordotonal organ of the locust leg exhibit much hysteresis. For a given joint angle, the ratio of an afferent's tonic firing rate after extension to its firing rate after flexion (or vice versa) is typically between 1.2:1 and 3:1 but can be as large as 10:1. Spiking local interneurons, that receive direct inputs from these afferents, can, by contrast, exhibit much less hysteresis (between 1.1:1 and 1.2:1). We tested the hypothesis that presynaptic inhibitory interactions between afferent axons reduces the hysteresis of postsynaptic interneurons by acting as an automatic gain control mechanism.

2. We used two kinds of neural models to test this hypothesis: *1*) an abstract nonspiking neural model in which a multiplicative, shunting term reduced the "firing rate" of the afferent and *2*) a more realistic compartmental model in which shunting inhibition presynaptically attenuated the amplitude of the action potentials reaching the afferent terminals.

3. The abstract neural model demonstrated the automatic gain control capability of a network of laterally inhibited afferent units. A postsynaptic unit, which was connected to the competitive network of afferents, coded for joint angle without saturating as the strength of the afferent input increased by two orders of magnitude. This was possible because shunting inhibition exactly balanced the increase in the excitatory input. This compensatory mechanism required the sum of the excitatory and inhibitory conductances to be much larger than the leak conductance. This requirement suggested a graded weighting scheme in which the afferent recruited first (i.e., at a small joint angle) received the largest inhibition from each of the other afferents because of the lack of active neighbors, and the afferent recruited last (i.e., at a large joint angle) received the least inhibition because all the other afferents were active.

4. The compartmental model demonstrated that presynaptic shunting inhibition between afferents could decrease the average synaptic conductance caused by the afferents onto the spiking interneuron, thereby counterbalancing the afferents' large average firing rates after movements in the preferred direction. Therefore the total postsynaptic input per unit time did not differ much between the preferred and nonpreferred directions. Hysteresis in the response of the modeled postsynaptic interneuron was thereby reduced from ratios as high as 2.5:1 to <1:1. In addition, shunting inhibition prevented the modeled interneuron from saturating and from failing to fire. A local, lateral interaction shunting scheme in which an afferent is shunted only by its nearest neighbors (i.e., those afferents that are recruited at similar angles) reduced hysteresis and maintained the dynamic range of the spiking interneuron better than a global interaction scheme, where all afferents are presynaptically connected to each other.

5. The results of these simulations demonstrate a potential role for the established presynaptic inhibitory interactions between proprioceptive afferent terminals. In addition, these results allow us to make several testable predictions. First, if lateral shunting inhibition between afferent terminals can be selectively blocked pharmacologically, hysteresis in the tonic response of the spiking local interneuron should increase. Second, presynaptic shunting inhibition should exist between afferents with similar recruitment thresholds, if not between all afferents that innervate the same spiking interneuron. Finally, we should expect a graded synaptic weighting scheme such that presynaptic inhibitory conductances are greater onto the afferents that are recruited early.

INTRODUCTION

Hysteresis is a widespread nonlinear phenomenon of most mechanosensory systems in which the activity of a neuron depends not only on the current state of the system but also on its recent history. In the cat it has been observed in the responses of muscle-spindle afferents and joint receptors (Kostyukov and Cherkassky 1992; Lennerstrand 1968), gravity-sensitive receptors in the vestibular system (Vidal et al. 1971), Pacinian corpuscles (Alvarez Buylla and Ramirez de Arellano 1953), and, in primates, at joint receptors (Grigg and Greenspan 1977). Hysteresis has also been observed in the activity of neurons that respond to head orientation in the lateral vestibular nucleus (Fujita et al. 1968) and in the thalamus for joint position of the limbs (Mountcastle et al. 1963). In invertebrates, hysteresis has been seen in the responses of the stretch receptors of the crayfish (Brown and Stein 1966; Chaplain et al. 1971; Segundo and Diez Martinez 1985), the propodite-dactylopodite joint proprioceptor of decapod crustaceans (Mill and Lowe 1972), the chordotonal afferents of the legs of the locust (Burns 1974; Matheson 1990, 1992), and nonspiking local interneurons of the locust (Siegler 1981).

Hysteresis presents a problem to the nervous system because proprio-and mechanoreceptors should transmit information faithfully about the current state of the periphery. Hysteresis distorts this transmission by making the firing rate of an afferent dependent on past events so that it does not code unambiguously for the current state. A given joint angle could be represented by many different firing rates, depending on the past movement of the joint. How does the nervous system overcome this problem, if at all?

We have studied this problem by focusing on hysteresis in the responses of afferents in the metathoracic chordotonal organ of the locust that signal the position of the femorotibial joint of the hind leg (Matheson 1990, 1992). Neurons with a maximum tonic response at flexed joint angles show a higher tonic firing rate for a given angle of the femorotibial joint if this angle is reached via flexion than via extension.

The reverse holds for afferents whose maximum tonic response occurs at extended joint angles. The property that the tonic activity of an afferent is larger after a movement in the direction of maximum response is actually quite common (Burns 1974; Kostyukov and Cherkassky 1992; Mill and Lowe 1972). On the basis of the published results of Matheson (1990, 1992), the ratio of tonic responses in the two directions ranges from 1.2:1 to 3:1 but can on occasion be as large as 10:1 near the middle of their response range (Matheson 1992). The tonic responses of afferents differ from each other in the joint angles at which they are recruited and the angles at which their tonic firing rates saturate.

The origin of this hysteresis could be mechanical, neuronal, or both. Mechanical hysteresis is a property of many nonlinear viscoelastic systems (Chaplain et al. 1971). The metathoracic femoral chordotonal organ lies in the distal region of the femur and is mechanically connected to the femorotibial joint by an elastic apodeme that buckles to form a loop when relaxed (i.e., when the femorotibial joint is extended) (Shelton et al. 1992). As the femorotibial joint is flexed, the apodeme is stretched, and the size of the loop is reduced. The size of the loop exhibits hysteresis, and the polarity of this hysteretic effect is consistent with the polarity of the hysteretic response of the chordotonal afferents. The stretching of the apodeme complex at a given joint angle is greater after a movement in the direction of greater tension, i.e., flexion.

Hysteresis could also result from membrane properties of the afferent neurons. Intracellular recordings from the receptor region of these neurons have not been made in conditions where current stimulation is used instead of mechanical stretching. It is thus, at this time, impossible to estimate the relative contributions of membrane and mechanical mechanisms.

Spiking local interneurons in the metathoracic ganglion are the primary integrators of incoming mechanosensory signals from the leg and receive monosynaptic inputs from chordotonal afferents (Burrows 1987). Their dynamic range can be very large (120°), whereas chordotonal afferents typically exhibit a limited dynamic range (range fractionation) (from 60 to 100°), suggesting that a given spiking interneuron receives inputs from a number of afferents, each with a different recruitment threshold. These interneurons show much less hysteresis than the afferents presynaptic to them. The average hysteresis in one carefully studied spiking interneuron was between 1.1:1 and 1.2:1 (Burrows 1985). What could account for this reduction in hysteresis? An apparent mechanism might simply be averaging the response of many afferents. This hypothesis is untenable because all afferents with similar tuning properties (i.e., maximum activity at either flexed or extended joint angles) exhibit hysteresis with the same polarity. Thus a particular spiking interneuron presumably receives inputs from afferents with similar tuning properties, and averaging would fail to eliminate hysteresis. It is difficult to imagine how an interneuron that responds maximally to extended joint angles would receive inputs from afferents that respond maximally to flexed joint angles. Whatever the mechanism, hysteresis does not seem to involve any intervening neuronal processing stages and most likely occurs locally somewhere between the central terminals of the chordotonal afferents and the dendritic processes of the spiking local interneuron.

We hypothesized that presynaptic shunting inhibition between afferent axons reduces hysteresis on the postsynaptic spiking local interneuron by acting as an automatic gain control mechanism (Grossberg 1973). Burrows and Laurent (1993) and Burrows and Matheson (1994) demonstrated experimentally the existence of presynaptic, shunting inhibition between afferents at axon terminals. Postsynaptic potentials (PSPs) are generated in the terminals of one afferent as a result of spikes in other afferents responding to the same movement. These synaptic potentials reverse at a membrane potential slightly positive to the resting potential (about −70 mV). These PSPs appear to be mediated by γ-aminobutyric acid (GABA) and must, therefore, be caused by interposed neurons because the afferents themselves are not GABAergic (Leitch et al. 1993; Sattelle and Breer 1990). These PSPs can shunt an orthodromic action potential for up to 100 ms after the onset of the PSP (Burrows and Laurent 1993) and, consequently, reduce the amplitude of the spike-evoked excitatory PSP (EPSP) in postsynaptic neurons (Burrows and Matheson 1994). We have demonstrated the possible function of such shunting inhibition by performing a number of simulations with the use of two kinds of neural models: an abstract, nonspiking model with leaky-integrator and shunting dynamics (Grossberg 1988) and a more realistic, compartmental model.

Abstract model

We use first a simplified, nonspiking dynamical model neuron to elucidate the mechanism by which presynaptic, shunting inhibition between afferents can act like an automatic gain control mechanism. The change in membrane potential depends on the sum of excitatory, inhibitory, and leak currents

$$C\dot{V}_i(t) = -G_{\text{leak}}V_i(t) + [E^+ - V_i(t)]G^+_{\text{rec}}(t) + [E^- - V_i(t)]G^-_{\text{syn}}(t) \quad (1)$$

where C is the membrane capacitance, G_{leak} is the membrane leak or passive conductance, E^+ and E^- are the excitatory and inhibitory reversal potentials respectively, $G^+_{\text{rec}}(t)$ is the excitatory receptor conductance change, $G^-_{\text{syn}}(t)$ is the inhibitory synaptic conductance change due to the activity of neighboring afferents, and $V_i(t)$ is the membrane potential of afferent i. According to this model, the resting potential is defined to be zero.

At equilibrium, the membrane potential becomes

$$V_i(\infty) = [E^+G^+_{\text{rec}}(t) + E^-G^-_{\text{syn}}(t)]/[G_{\text{leak}} + G^+_{\text{rec}}(t) + G^-_{\text{syn}}(t)] \quad (2)$$

Two assumptions can be made to constrain the relative values of the parameters in *Eq. 2*. First, to provide adequate gain control, the leakage conductance must be much smaller than the sum of the excitatory and inhibitory conductances. Second, the contribution of the inhibitory conductance to the membrane voltage should not swamp that of the excitatory conductance in the numerator of *Eq. 2*, which requires the inhibitory reversal potential be close to the resting potential (i.e., $E^- = 0$). The first assumption has not been tested experimentally in this system, although much smaller values for neuronal leak membrane conductance have been recently reported (Major et al. 1990; Spruston and Johnston 1991). The second assumption has been supported experimentally (Burrows and Laurent 1993). Given these two assumptions,

the equilibrium membrane potential becomes proportional to the ratio of the excitatory to the total synaptic conductance

$$V_i(\infty) = E^+ G^+_{\text{rec}}(t)/[G_{\text{tot}}(t)] \quad (3)$$

where $G_{\text{tot}}(t)$ is the sum of the excitatory and inhibitory conductances. This provides an automatic gain control or self-normalizing mechanism. If the strength of the excitatory inputs to all neurons in the competitive network is increased by some factor and the neurons are operating near the linear region of their transfer functions (i.e., the function relating the voltage at the spike-initiation zone to the firing rate), the membrane potential of any given neuron will not saturate but rather will remain invariant because the inhibitory conductances from neighboring afferents will increase by the same factor (Grossberg 1973). Therefore the ratio of excitatory to total input conductance will not change.

Compartmental model

As a more realistic model of the electrical properties of a neuron and its interactions with other neurons, the compartmental model reveals one important shortcoming of the abstract model. Shunting inhibition acts at the afferent terminals by attenuating the amplitude of an invading action potential, and not by modulating the firing frequency. The amplitude and duration of the action potential, in turn, determine the magnitude and time course of voltage-dependent calcium conductances that determine the amount of released transmitter (Smith and Augustine 1988). Thus shunting inhibition affects the magnitude of each synaptic event.[1] The total synaptic input per unit time from a given afferent to the postsynaptic interneuron is equal to the product of its firing rate and the average magnitude of each synaptic event. Let us assume that the pattern of firing across the set of N afferents innervating a given spiking interneuron can be represented by the following vector

$$\hat{f} = (f_1, f_2, \ldots, f_N) \quad (4)$$

By assuming that shunting synaptic conductances are dominant at the afferent terminal, the amplitude of an action potential from afferent i, V_i, arriving at the terminal is inversely proportional to the total shunting conductance per unit time

$$V_i \propto \left(\sum_{j=1}^{N} f_j a_{ij}\right)^{-1} \quad (5)$$

where a_{ij} is the synaptic gain of the shunting synapse from afferent j onto afferent i. The average magnitude of a synaptic event from afferent i onto the postsynaptic interneuron is related to the afferent's spike amplitude by a synaptic transfer function, $g(x)$. Therefore the total synaptic input per unit time onto the interneuron from afferent i, input$_i$ is

$$\text{input}_i \propto f_i g(V_i) \quad (6)$$

If $g(x)$ is linear, any gain change in the firing pattern of the afferents will be compensated for by the shunt, and input$_i$ will remain unchanged. In reality, the synaptic transfer function is not linear, and so gain control will not work ideally, particularly for very large gain changes in the firing pattern.

[1] If shunting synapses occurred near branch points of the afferent terminal, they could prevent spikes from invading particular terminal branches, thereby decreasing the number of active release sites. Therefore shunting inhibition could also affect the number of synaptic events. For simplicity, we have modeled the afferent terminal as a single process so that shunting inhibition does not affect the number of synaptic events.

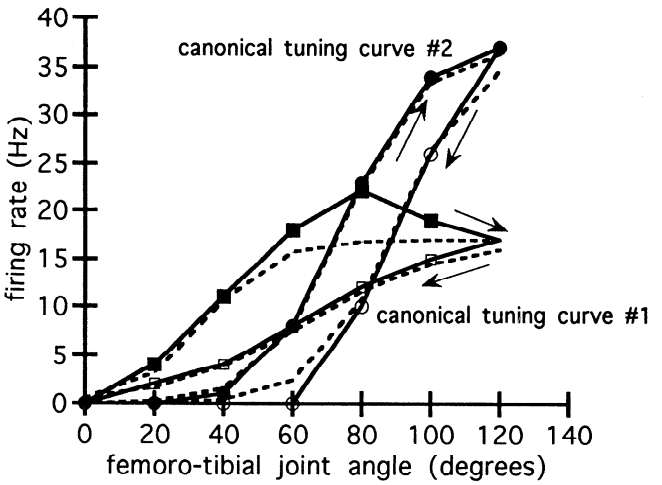

FIG. 1. Tuning curves of 2 afferents (——) with maximum responses at extended joint angles copied from Matheson (1992) and the canonical curves (– – –) based on Boltzmann functions that were used to model them.

Hysteresis reduction

This automatic gain control mechanism can be used to reduce hysteresis. If we assume that a group of afferents with similar tuning curves form a competitive network of mutual shunting inhibition, hysteresis will change the excitatory conductances to each neuron in the group in a similar manner (i.e., either increase or decrease them). In so far as hysteresis can be treated as a similar gain change across all the excitatory inputs, this automatic gain control mechanism will act to eliminate the hysteresis at the axon terminals. In reality, hysteresis cannot always be treated as a pure change in gain, and it may not be exactly uniform across the set of afferents. In addition, the synaptic transfer function is linear only within a small domain of its operating range. Therefore, in reality, we should expect to see only a reduction and not a total elimination of hysteresis over all joint angles.

METHODS

Abstract model

A simplified, nonspiking network model was used that consisted of 13 units: 12 "afferent" units that mutually inhibited one another, and a single "interneuronal" unit that received excitatory connections from the other 12 units. The dynamics of each of the afferent units followed a first-order, shunting equation (Grossberg 1988) much like *Eq. 1*, except that the inhibitory conductance is replaced with a weighted sum of the inhibitory inputs and the inhibitory reversal potential is set to zero

$$C\dot{V}_i = -G_{\text{leak}} V_i(t) + (E^+ - V_i) G^+_{\text{rec}}(t) - V_i \sum_{j \neq i} w_{ij} f(V_j) \quad (7)$$

where w_{ij} is the inhibitory weight between units i and j, and $f(x)$ is the transfer function mapping the summated, dendritic, membrane voltage to the firing rate. The set of 12 ordinary differential equations were either numerically integrated for 1 s with the use of a

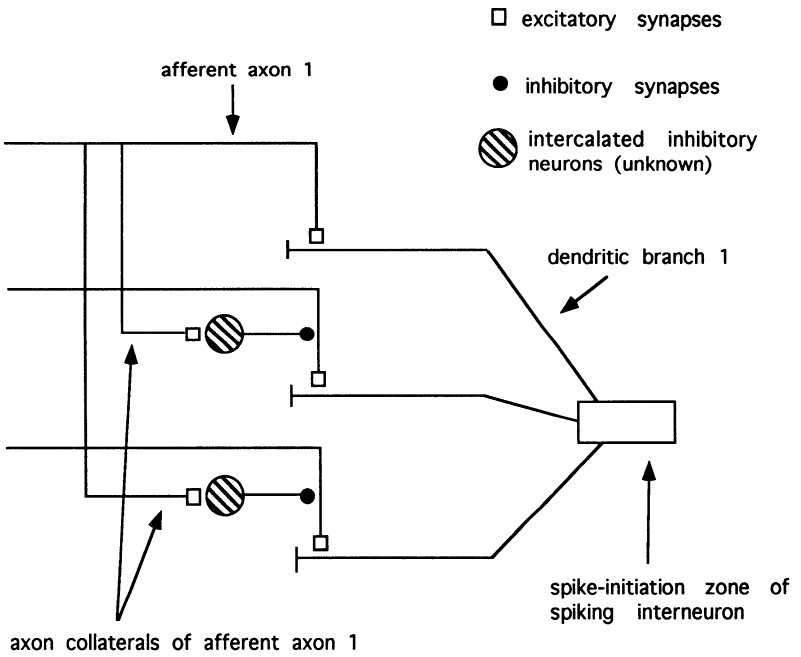

FIG. 2. Schematic diagram of the presumed presynaptic inhibitory connections between afferents and of their excitatory connections onto a spiking local interneuron (see Burrows 1987; Burrows and Laurent 1993; Burrows and Matheson 1994).

fourth-order, Runge-Kutta integrator with a fixed time step of 1 ms or solved algebraically at equilibrium.

Inputs to the afferent units were simulated as step changes in excitatory conductance. To determine their values, the tuning properties of two representative afferents recorded by Matheson (1992) were fit to Boltzmann functions to be used as canonical curves (Fig. 1). Hysteresis of the first afferent involved both a horizontal shift and a change in slope, the combination of which mimics a simple gain change (canonical tuning curve #1). Hysteresis of the second afferent was modeled as a horizontal shift of its tuning curve (canonical tuning curve #2). Hysteretic ratios for both afferents peaked at values between 2.5:1 and 3:1 near the middle of their dynamic ranges. The inverse of these tuning curves were used to map afferent firing rates to femorotibial angles. The value of $G^{+}_{\text{rec}}(t)$ was made proportional to the femorotibial joint angle.

Compartmental model

A more realistic, compartmental model was designed in which the cable properties of the intracellular space and membrane, and the kinetics of various voltage-dependent channels were modeled, with the use of the NEURON simulator (Hines 1989). A set of 12 single-compartment afferent axons was simulated.[2] In turn, each of these axons made synapses onto a passive dendrite that funneled inputs into an active region representing the spike-initiation zone of the spiking local interneuron (Fig. 2). The presynaptic inhibition at the axon terminals is mediated by interposed neurons that are so far unidentified (Burrows and Laurent 1993). Because nothing is known about these interposed neurons, axonal collaterals from each afferent axon were used to simulate lateral inhibition between the afferent axons. Except for a small synaptic time delay, the addition of these neurons in our model would not have affected the results of these simulations. Therefore the complete model was composed of 145 active compartments (12 afferent axons × 12 collaterals per axon + 1 spike-initiation zone of the interneuron) and 12 passive compartments (the 12 dendrites of the interneuron). The lengths and diameters of all compartments were within known anatomic ranges (Table 1).

Each axon compartment was composed of one passive conductance (G_{leak}), three voltage-dependent conductances (G_{Na}, G_{KDR}, and G_{KA}), and two synaptic conductances [excitatory: $G^{+}_{\text{syn}}(t)$ and inhibitory: $G^{-}_{\text{syn}}(t)$; Fig. 3. The sodium conductance and "delayed-rectifier" potassium conductance followed Hodgkin-Huxley kinetics and formed the basic spiking mechanism for the afferents and spiking local interneuron (Hodgkin and Huxley 1952). An additional "A"-type potassium conductance (Hagiwara et al. 1961) was added to the active compartments to generate low firing rates, as observed in chordotonal afferents (Matheson 1992) and spiking interneurons (Burrows 1985). This conductance provided lower firing rates by slowing the decay of afterhyperpolarization (Connor and Stevens 1971; Rogawski 1985). The model's A-type conductance followed first-order kinetics with equilibrium activation, $m(\infty)$, and inactivation, $h(\infty)$, values obeying a Boltzmann function parameterized by k and $V_{1/2}$

$$m(\infty) = 1/[1 + e^{-k_m(V - V_{1/2_m})}] \quad (8)$$

$$h(\infty) = 1/[1 + e^{-k_h(V - V_{1/2_h})}] \quad (9)$$

The channel conductance was a time- and voltage-dependent function of the activation and inactivation variables

$$g(t, V) = g_{\max} m^3(t, V) h(t, V) \quad (10)$$

where $g_{\max}$ is the maximum conductance (see Table 2).

Table 3 lists the maximum conductances and reversal potentials for all active and passive channels. Figure 4 shows the firing rate

TABLE 1. *Physical dimensions used in compartmental model*

	Afferent Axons and Collaterals	Interneuronal Dendrites	Interneuronal Spike-Initiation Zone
Length, μm	30,000	200	100
Diameter, μm	4	3	10

[2] A compartment is defined as a section of cable with a particular length, diameter, and set of voltage-dependent conductances. The number of segments determines the number of isopotential subsections along the compartment. In our simulations, each compartment consisted of three isopotential segments: one at the beginning, one in the middle, and one at the end of the compartment.

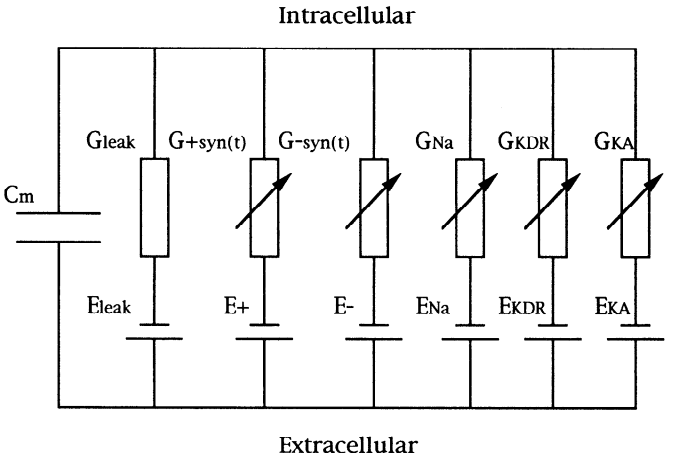

FIG. 3. Diagram of the components in 1 compartment of the realistic model of an afferent. Each compartment is composed of a capacitor (C_m) in parallel with a leakage conductance (G_{leak}), excitatory and inhibitory synaptic conductances [$G^{+}_{syn}(t)$ and $G^{-}_{syn}(t)$], and 3 active conductances (Na, delayed-rectifier K, and "A" K conductances) used to generate spiking.

of one of the model's afferents as a function of DC current input. Note the existence of firing rates well below 10 Hz for smaller input currents. The dynamics were numerically integrated for 1 s with the use of the backward, Euler method with a fixed time step of 25 μs (Press et al. 1990).

Inputs

Excitation of the afferent axons due to stretch or relaxation of the chordotonal organ was simulated with current inputs rather than with receptor conductance changes. This is a justified simplification because of the large distance (>3 cm along axons whose diameter is <5 μm in adult locusts) separating the site of generation of the receptor potential from the axonal terminals where shunting inhibition and transmitter release occur. Therefore inputs reaching the axonal terminal could be treated as pure current sources, independent of membrane voltage at the terminal. To determine appropriate tonic current inputs for each afferent axon, the following procedure was adopted. First, the current-frequency relationship of the simulated afferent was measured and fit piece-wise with a set of second-order polynomial functions. Second, the two canonical tuning curves described in Fig. 1 were used to map femorotibial joint angle to firing rate. Finally, the polynomial and Boltzmann functions were composed to map joint angle to tonic current input. Thus the model afferents possessed tuning curves that matched those of actual afferents regardless of whether the current-frequency curves of the model afferents matched. Unless otherwise noted, the tuning curves of the afferents used in any particular simulation were horizontally shifted versions of one of the canonical tuning curves. This was done to simulate the finding that the afferents exhibit a range of joint angles at which they are recruited (Matheson 1992).

TABLE 2. *Activating and inactivating kinetics of A-type potassium channel*

	Activating	Inactivating
$V_{1/2}$, mV	−77	−77
k, mV^{-1}	−35	8
Time constant, ms	1	1 or 50 if V is less than −65 mV

The steady-state values of activation and inactivation are parameterized with the use of a Boltzmann function with half-maximum voltage, $V_{1/2}$, and slope, k, parameters. Also listed are the time constants of the first-order kinetics. Notice how the inactivating kinetics slow down considerably if the membrane voltage falls below −65 mV.

TABLE 3. *Passive and active channel characteristics used in compartmental model*

	Leak	Sodium	DR Potassium	A Potassium
Maximum conductance, S/cm^2	0.00005	0.30	0.072	0.5
Reversal potential, mV	−65 or −54.3	50	−77	−77

DR, delayed rectifier.

To prevent synchrony between spikes in different axons, the onsets of current injections were staggered randomly within a time window of 200 ms. Two other forms of noise were added. First, uniformly distributed current noise with a zero mean and range of 1 ± 0.67 (SD) nA was introduced into the afferent axons and collaterals and the spiking interneuron. Second, the magnitude of each synaptic conductance change was randomly perturbed with a uniformly distributed conductance of zero mean and range of 10 ± 6.67% of the unperturbed conductance.

Every time an action potential was registered at the terminal of an axon or collateral, a "synaptic" event was triggered. This synaptic event (i.e., postsynaptic conductance) was described by an alpha function (Rall 1967). The time-to-peak values for the excitatory and shunting inhibitory synaptic conductances were 6 and 15 ms, respectively, unless otherwise stated. These values correspond to conductance durations of ~18 and 45 ms, respectively, and are constrained by physiological data. Siegler and Burrows (1983) found that one class of excitatory synaptic conductances onto spiking local interneurons lasted 15 ms. Burrows and Laurent (1993) inferred that the duration of shunting inhibitory conductances could range from 25 to 100 ms. The peak value of the postsynaptic conductance, g_{peak}, depended exponentially on the amplitude of the presynaptic action potential, V_{amp}

$$g_{peak} \propto e^{\beta V_{amp}} \qquad (11)$$

where β was set to 0.164 (Katz and Miledi 1967).

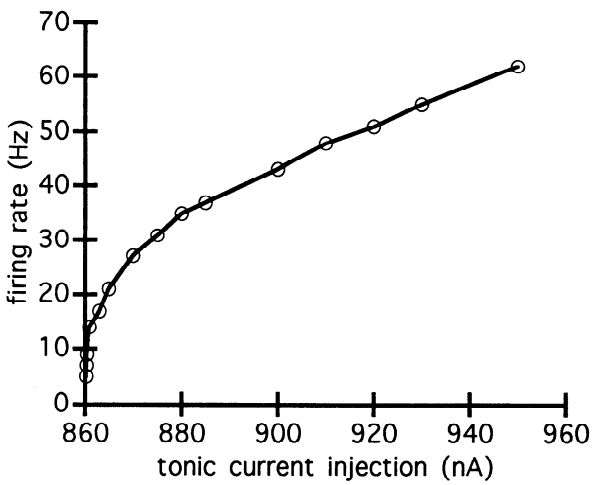

FIG. 4. Frequency-current (F-I) curve of 1 of the afferent axons in the compartmental model. The curve is linear for most of the current range except for low currents. Large currents were required to obtain spiking because of the lack of simulated, insulating myelin, which would decrease current leakage and membrane capacitance. The size of this current is irrelevant to the study of hysteresis reduction.

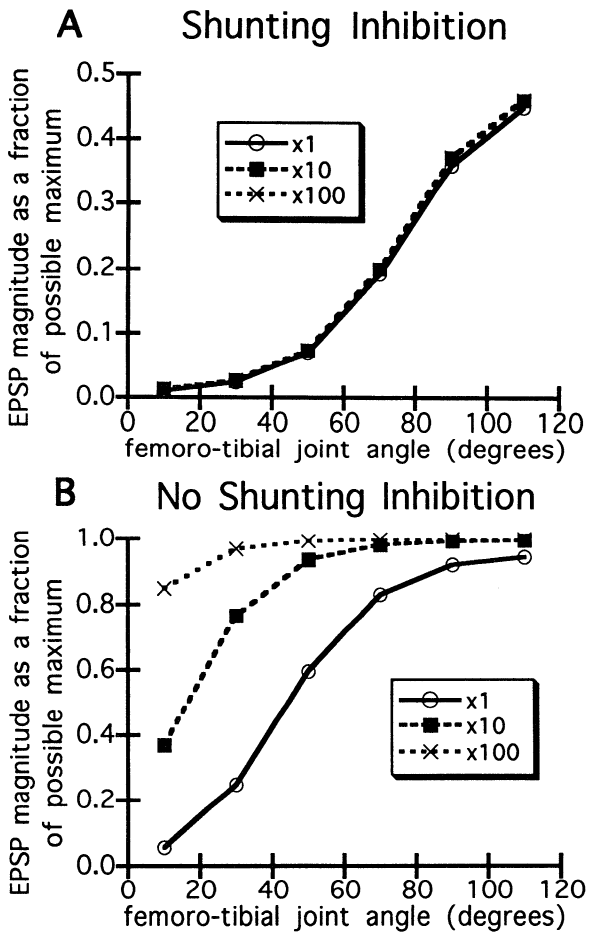

FIG. 5. Activity of the modeled postsynaptic interneuron as a function of femorotibial joint angle. Activity is represented by the excitatory postsynaptic potential magnitude as a proportion of the maximum possible value. *A*: with shunting inhibition, the interneuron codes for joint angle even when the gain of the excitatory input is increased by 2 orders of magnitude. *B*: without shunting inhibition, the interneuron saturates at the reversal potential of its excitatory synaptic conductance. It is unable to adapt to increasing input amplitudes.

RESULTS

Abstract model

These first simulations showed that a competitive shunting network can adjust its gain automatically and thereby operate without saturation when confronted with excitatory inputs whose magnitudes vary by several orders of magnitude. Figure 5*A* shows the membrane potential of the local interneuron as a function of femorotibial joint angle for three different input levels (×1, ×10, ×100). The input levels were increased by multiplying the receptor conductance, $G^{+}_{\text{rec}}(t)$, by one of these three factors while keeping all the other parameters in *Eq. 7* constant. The strength of the inputs varied by two orders of magnitude, and yet the local interneuron was able to encode joint angle in a nearly identical fashion in all circumstances. Shunting inhibition exactly counterbalanced the variations of excitatory input level (see *Eq. 3*). Figure 5*B* shows the consequences of removing shunting inhibition between afferent terminals. The local interneuron's activity saturated, and its dynamic range decreased as the strength of the input was increased.

These simulations suggested that some weighting schemes are more appropriate than others. The model's afferents that are recruited first (i.e., with low angular recruitment thresholds) receive inhibition from only a few neighboring afferents at small joint angles. Because the total synaptic conductance must be much larger than the leakage conductance to generate adequate gain control, the shunting weights to these afferents should be large enough to compensate for the lack of active neighbors. On the other hand, those afferents that are recruited only at very large joint angles will receive inhibition from many more active afferents, and so weights to them should be smaller to prevent extreme inhibition.

Compartmental model

To determine whether hysteresis could arise solely from the biophysical properties of the model afferents, current was injected into the model afferent, and after a short holding period it was either increased or decreased. After an additional holding period, the level of the injected current was returned to its original value. This was repeated with a large number of starting values over the dynamic range of the model afferent, and with a variety of increments and decrements. In some cases, we noticed a small amount (as much as 6%) of hysteresis in the afferent firing rate in the first 100 ms but never afterward. These simulations suggested that very little of the experimentally observed hysteresis that occurs over 1–3 s (Matheson 1992) could be simulated by the biophysical properties of the model afferents alone. Therefore the hysteresis was simulated by varying the input current to each afferent as a function of its past history (i.e., the preceding movement). Of course, these simulations do not provide evidence against the biophysical origins of hysteresis because the model afferents do not necessarily contain all the critical membrane properties of the biological afferents. The detailed membrane properties of these proprioceptive afferents are unknown. The purpose of this study was to provide a neurally plausible algorithm by which hysteresis could be reduced and not to provide an explanation for the origins of hysteresis.

Two variables were used to assess the degree of hysteresis of the interneuron. First, the total synaptic input to the spiking interneuron was defined as the product of the number of synaptic events per second and the average peak synaptic conductance. Second, the firing rate of the interneuron was measured as the number of overshooting action potentials per second after the first 100 ms to avoid any transient response. The total synaptic input was a more reliable variable because small overshooting spikelets were often observed but generally not included in the measurement of the firing rate. Moreover, the interneuron would often saturate and fail to fire when shunting inhibition between afferent terminals was weak or absent. Very large intracellular current injections will often cause the biological interneuron to stop firing (personal observation).

The tonic firing rates of the model's 12 afferents after extension and flexion are shown in Fig. 6. These curves were produced by shifting laterally the first canonical tuning curve (Fig. 1). A local gradient weighting scheme was used, such that each afferent received presynaptic inhibition from its two nearest neighbors (1 on each side) only (where neighbor

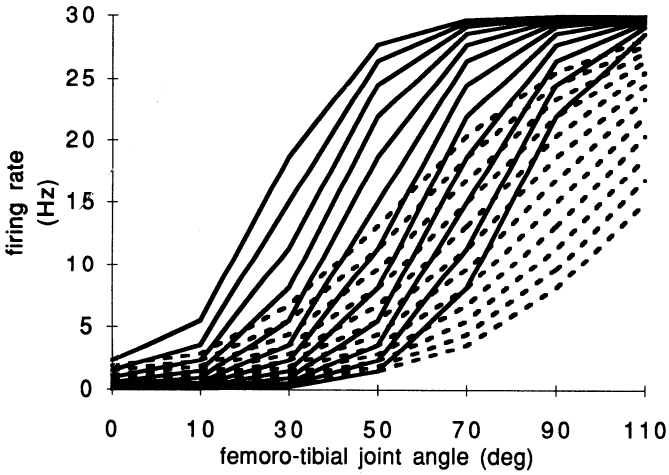

FIG. 6. Tuning curves of the 12 afferents after flexion (– – –) and extension (——) used in the 1st set of simulations using the compartmental model. Each pair of curves is shifted horizontally by 7° with respect to its neighbor.

is defined as similarity of the recruitment threshold). A given afferent thus received inhibition from the afferents that were recruited at joint angles slightly smaller and larger than its own recruitment threshold. In addition, the weights of the synapses to the afferent recruited first were larger than those to the afferent recruited at larger angles. The particular set of weight values was chosen to produce adequate performance in terms of hysteresis reduction. A thorough search through weight space could not be performed because of limits in computational time. However, on the basis of a number of simulations in which the weights were varied, the model's performance was robust such that hysteresis reduction did not depend critically on a particular set of weights. Total synaptic input versus joint angle is plotted in Fig. 7 with and without shunting inhibition between afferent terminals. First, shunting inhibition attenuated the total input to the interneuron by as much as 85% and was essential to maintain its membrane potential within a range where spiking could occur (Fig. 8, *Aiv–Avi*). If shunting interactions between afferent terminals were suppressed, the firing rate of the interneuron became unable to encode joint angles >70° (Fig. 9, *Aiv–Avi*).

Second, hysteresis [as measured by the postsynaptic conductance (Fig. 7) or the firing rate of the interneuron (Figs. 8 and 9)] was greatly reduced by shunting interactions between afferent terminals. For example, if shunting inhibition was present, the firing rate was 20 Hz after both extension (Fig. 8*Aiv*) and flexion (Fig. 8*Biv*) when the leg was held at 70°. By contrast, if interactions between afferents were suppressed, the firing rate of the interneuron was ~4 Hz after an extension (Fig. 9*Aiv*) and ~22 Hz after a flexion (Fig. 9*Biv*). The tonic firing rates of the interneuron after flexion or extension are plotted in Fig. 10 when shunting inhibition was present.

To quantify the reduction in hysteresis due to shunting interactions between afferent terminals, the ratio of the response of the interneuron after extension to that after flexion was computed as a function of joint angle and

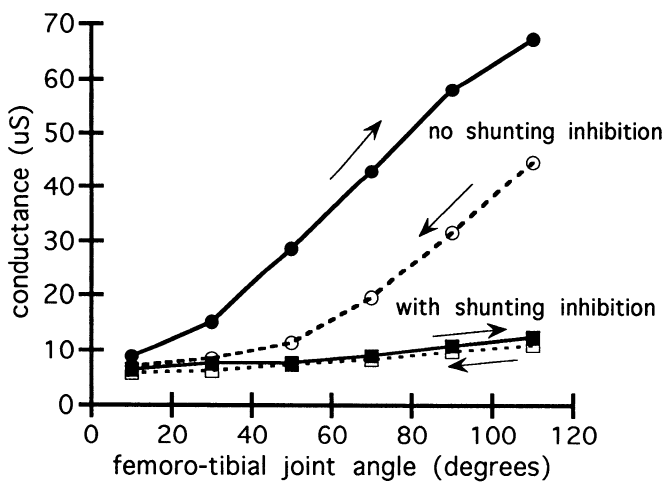

FIG. 7. Total synaptic input to the simulated spiking interneuron as a function of joint angle with and without shunting inhibitory interactions between the afferents. Solid lines represent total synaptic inputs in the extension direction, and dashed lines represent total synaptic inputs in the flexion direction. Total synaptic input is defined as the product of the number of synaptic events per second and the average peak conductance of each event.

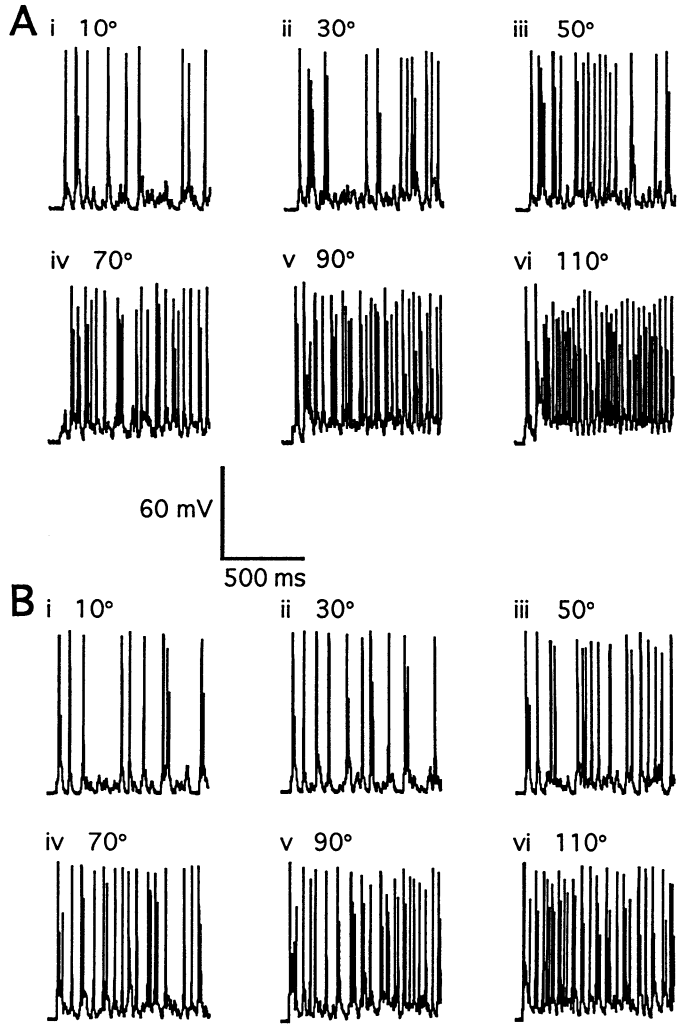

FIG. 8. Transmembrane voltage of the simulated spiking interneuron, as recorded from the center of its spike-initiation zone, for each of 6 joint angles in the extension direction (*Ai–Avi*) and in the flexion direction (*Bi–Bvi*). There is presynaptic shunting inhibition between afferent terminals.

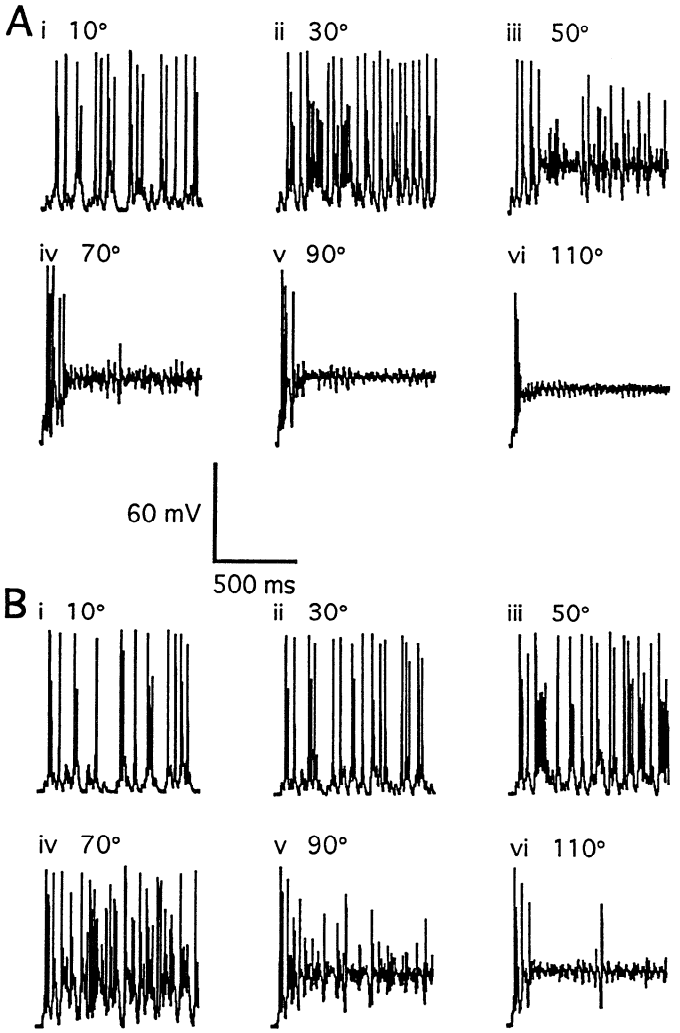

FIG. 9. Transmembrane voltage of the spiking interneuron, as recorded from the center of its spike-initiation zone, for each of 6 joint angles in the extension direction (*Ai–Avi*) and in the flexion direction (*Bi–Bvi*). There is no presynaptic shunting inhibition between afferents terminals. Note both saturation and hysteresis. Compare with Fig. 8.

called the hysteretic ratio (Fig. 11*A*). A ratio of 1.00 represents total elimination of hysteresis, and a ratio <1.00 represents a reversal in hysteresis such that the interneuron responds more strongly after flexion than after extension despite the fact that the afferents respond in the opposite manner. The hysteretic ratio was uniformly low with shunting inhibition. On the other hand, the hysteretic ratio peaked at a joint angle of 50° without shunting inhibition. At this joint angle, the hysteretic ratio was almost two and a one-half times larger without shunting inhibition. The average hysteretic ratio (averaged over all joint angles between 0 and 180° and measuring total synaptic input) was 1.11 with shunting inhibition and 1.85 without shunting inhibition. The average hysteretic ratio was 1.03 and 1.09 (measuring the firing rate of the interneuron and with the use of window thresholds of 0 and −30 mV, respectively)[3] with shunting inhibition. These simulations were performed five times (each time with a different random number seed; the random number seed determined the particular sequence of random numbers used to model noise). The average hysteretic ratio (averaged over all 6 joint angles and 5 simulations) was 1.12 with shunting inhibition versus 1.63 without (Fig. 11*B*). The difference between the hysteretic ratios with and without shunting inhibition was highly significant [$t(4) = 76.98$, $P < 0.005$].

The principle underlying hysteresis reduction can be made clearer by considering the pattern of afferent inputs to the local interneuron. The total postsynaptic conductances delivered by all 12 afferents at each of 6 joint angles during extension (*A*) and flexion (*B*) are plotted in Fig. 12 (without shunting inhibition) and in Fig. 13 (with shunting inhibition). In these representations the total synaptic input to the interneuron is proportional to the area under each curve. In the absence of shunting inhibition, this area is much smaller (50% smaller at a joint angle of 110°) after a flexion (Fig. 12*B*) than it is after an extension (Fig. 12*A*). By contrast, because shunting inhibition acts to suppress most of the afferent inputs, such differences were reduced at most joint angles (Fig. 13).

A number of additional simulations were conducted to ensure that the results were not unique to the particular tuning properties of the model afferents. First, we performed two simulations in which the tuning curves were not only horizontally shifted but also scaled versions of canonical tuning curve #1. In the first simulation the saturation frequency was made proportional to the recruitment threshold. That is, the afferent with the largest recruitment threshold also saturated at the largest firing frequency. The average hysteretic ratio, based on total synaptic input, was 1.13 with shunting inhibition versus 1.67 without. In the second simulation the saturation frequency for each of afferents was randomly chosen. In this case the average hysteretic ratio, based on total synaptic input, was 1.16 with shunting inhibition versus 1.29 without.

Second, we tested the model with a set of afferents whose responses were described by canonical tuning curve

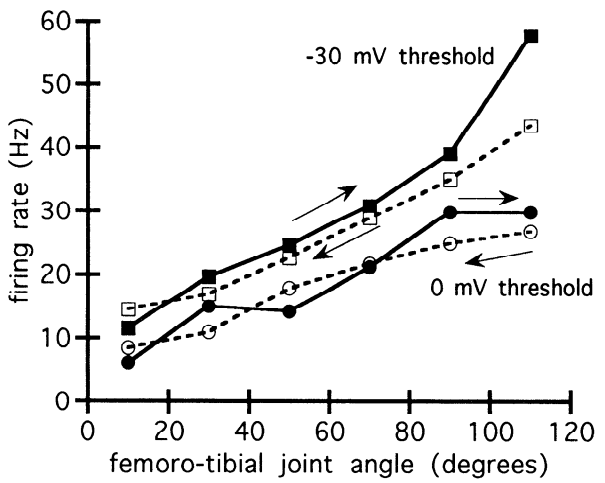

FIG. 10. Firing rate of the interneuron as a function of joint angle in the extension direction (——) and the flexion direction (– – –). Firing rate was estimated by counting the number of spikes above a threshold voltage of −30 mV (square markers) or 0 mV (circular markers). There is presynaptic shunting inhibition between the afferent terminals.

[3] These thresholds represent the voltages which a spike needs to exceed before it is counted in the average firing rate.

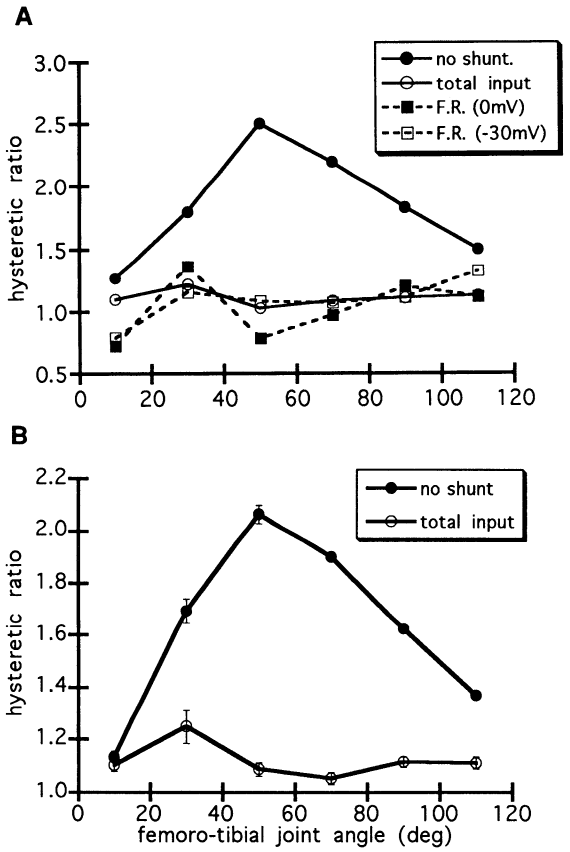

FIG. 11. Hysteretic ratio of the spiking interneuron's response as a function of joint angle. Hysteretic ratio is defined as the ratio of the response in the extension direction to that in the flexion response. *A*: response is defined as either total synaptic input (●, without shunting inhibition; ○, with shunting inhibition) onto or firing rate (■, 0-mV threshold with shunting inhibition; □, −30-mV threshold with shunting inhibition) of the postsynaptic interneuron. *B*: hysteretic ratios are averaged over 5 simulations, each with a different random number seed. Average hysteretic ratios with shunting inhibition (○) are based on total synaptic inputs to the postsynaptic interneuron. Average hysteretic ratios without shunting inhibition (●) are computed by taking the average of the ratios of the number of synaptic events in the extension direction to those in the flexion direction over the 5 simulations with shunting inhibition. This was done so that a paired *t*-test on the difference of hysteretic ratios with and without shunting inhibition could be performed. This assumes that the difference between the ratio of the total synaptic inputs and the ratio of the number of synaptic events is due primarily to the effects of shunting inhibition. This also saved computational time because an additional set of simulations without shunting inhibition was not required. Error bars indicate standard errors.

#2 (see Fig. 1). Hysteresis was then characterized mainly by a horizontal shift of the tuning curve rather than a change in slope. Because this does not represent a pure change in gain, we expected the results to be poorer than those from the initial simulations. Nevertheless, the average hysteretic ratio, as measured from the total synaptic input, was 1.10 with shunting inhibition and 1.28 without. Finally, we tested the model with two other afferent tuning curves transcribed from Matheson's (1990, 1992) studies (see Table 4). The model was able to reduce hysteresis in all cases, even when using inhibitory weight parameters that had been optimized for canonical tuning curve #1. It appears, therefore, that hysteresis reduction by lateral shunting inhibition occurs (although to a lesser extent) even under hysteretic conditions that are not characterized by simple gain changes.

Extent of inhibition

Hysteresis reduction depends on the number of inhibitory connections. The average hysteretic ratio (pooled over joint angles) decreased as a quadratic function of the number of neighbors, but the total amount of inhibition increased with the number of neighbors. In other words the total magnitude of inhibition is a confounding factor that covaries with the number of neighbors. The magnitude of the inhibitory weight from each neighbor must be scaled so that the total inhibition remains relatively constant despite changes in the number of neighbors. Normalizing the weighting of the inhibitory synapses indicated that a local weighting scheme (1 neighbor on each side) performed better than a global scheme in which each afferent received inhibition from all others. With 1 neighbor on each side, the average hysteretic ratio measured from interneuronal firing rates was 1.03 as opposed to 1.29 for 3 neighbors and 1.18 for 5 neighbors.

One reason for the superior performance of the local weighting scheme may be that the effect of the nonlinearity

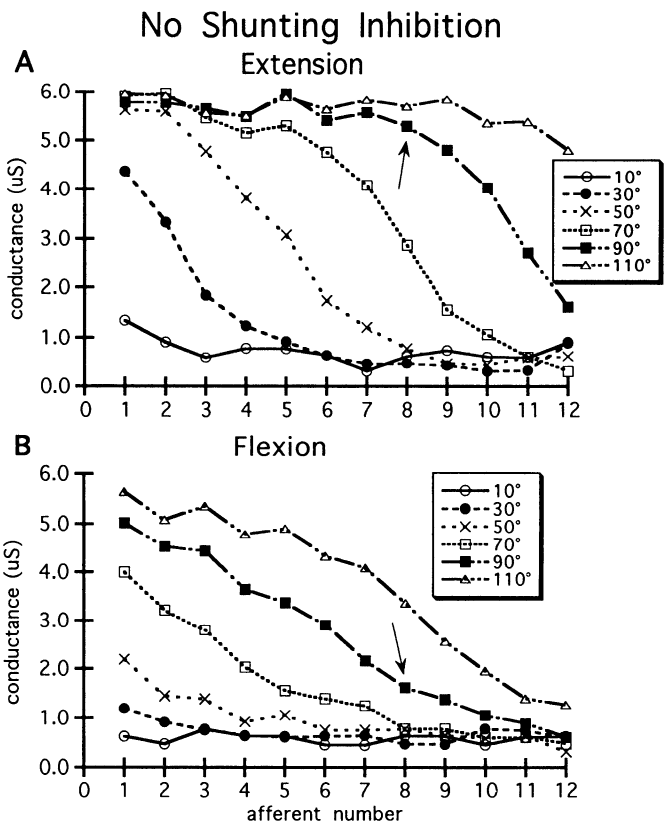

FIG. 12. Postsynaptic conductance changes evoked in the interneuron by the afferents (numbered 1–12) at each of 6 joint angles in the extension and flexion directions in the absence of presynaptic shunting inhibition. Postsynaptic conductance change is defined as the product of the number of synaptic events per second and the average peak conductance of each synaptic event at the postsynaptic interneuron from a single afferent. *A* and *B*: abscissa represents afferent identity. *Afferent 1* is recruited at the most flexed joint angles, whereas *afferent 12* is recruited at the most extended joint angles. Each symbol, therefore, represents the postsynaptic conductance change evoked in the interneuron by each corresponding afferent for a given joint angle. *A*: joint angle is arrived at during an extension. *B*: angle is arrived at during a flexion. The point indicated by an arrow, for example, indicates that *afferent 8* evokes a conductance change of 5.28 μS in the interneuron after an extension (*A*) and 1.63 μS after a flexion (*B*) when the leg is at 90°.

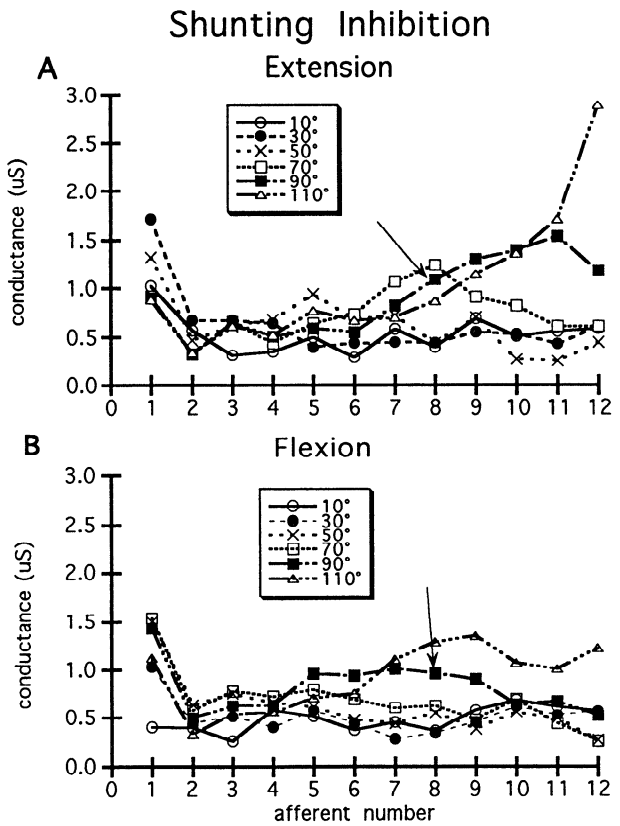

FIG. 13. Postsynaptic conductance changes evoked in the interneuron by the afferents (numbered 1–12) at each of 6 joint angles in the extension and flexion directions in the presence of presynaptic shunting inhibition. *A*: joint angle is arrived at during an extension. *B*: angle is arrived at during a flexion. The point indicated by an arrow, for example, indicates that *afferent 8* evokes a conductance change of 1.09 μS in the interneuron after an extension (*A*) and 0.96 μS after a flexion (*B*) when the leg is at 90°. Notice how the ratio of these 2 conductance changes is much smaller than the corresponding ratio in the absence of presynaptic shunting inhibition (see Fig. 12).

of neighboring afferents' tuning curves was minimized. Local neighbors have recruitment thresholds that are similar and so saturate at similar joint angles. Therefore, within the operating range of any given afferent, the responses of its local neighbors will remain relatively linear. This, on the other hand, is not true for distant neighbors that will either not be firing, or be firing at a saturated level for most of the operating range of the afferent in question. These nonlinearities will affect the automatic gain control mechanism and, therefore, will hinder the hysteretic reduction capabilities of shunting inhibition.

TABLE 4. *Average hysteretic ratio of interneuron using two other afferent tuning curves*

	Maximum Firing, Hz (Extend/Flex)	k, deg^{-1} (Extend/Flex)	With Shunting	No Shunting
Afferent 3	21/21	0.082/0.086	1.09	1.21
Afferent 4	16.6/21.06	0.177/0.034	1.05	1.10

These tuning curves are modeled as Boltzmann functions with maximum firing rate and slope, k, parameters.

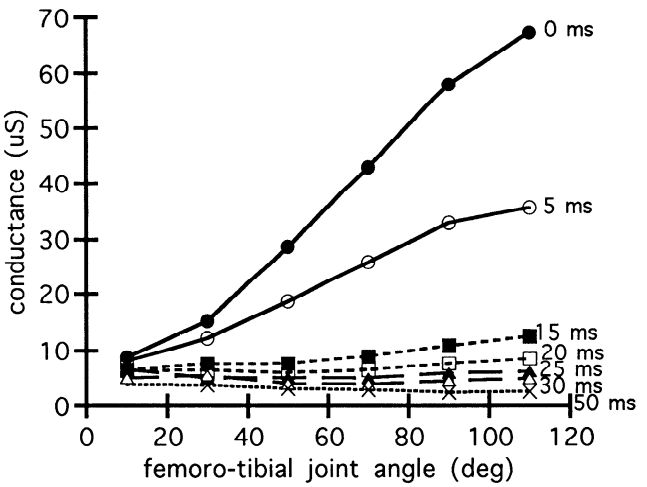

FIG. 14. Total postsynaptic conductance onto the interneuron in the extension direction as a function of joint angle for 7 inhibitory, synaptic time courses. Time course is measured as the time-to-peak of the synaptic conductance.

Parameter sensitivity

Mechanical hysteresis depends on the viscoelastic properties of the tissue of the proprioceptive organ and will vary with growth, use, or injury so that hysteretic reduction must be an adaptive process. Two parameters in the model can be varied to alter the degree of hysteretic reduction. First, varying the time-to-peak of the inhibitory synaptic conductance from 5 to 50 ms,[4] resulted in a monotonic drop in the hysteretic ratio (averaged over joint angles between 0 and 120°) from 1.6 to 0.83 (Fig. 14). Note that the slope of these curves is positive for time-to-peak values <25 ms and is negative at time-to-peak values >30 ms. This implies that the tuning curve of the interneuron will change polarity as the time-to-peak of the synaptic conductance increases above a certain level. Second, increasing the peak magnitude of all inhibitory synaptic conductances by a factor of 3 caused a drop in hysteretic ratio of ~30%. The time integral of each shunting synaptic conductance defines the magnitude of inhibition and is proportional to the product of the time-to-peak and the peak conductance magnitude. The hysteretic ratio decreases as a quadratic function of this product (Fig. 15).

DISCUSSION

We have shown with the use of numerical simulation techniques that a simple, biologically realistic, adaptive control mechanism can prevent synaptic saturation in mechanosensory circuits. An abstract, nonspiking model demonstrated that presynaptic shunting inhibition preserves the tuning properties of a spiking interneuron when the average input level increases by preventing saturation of its dendritic membrane potential. A compartmental model incorporating realistic membrane voltage and channel dynamics showed that presynaptic shunting inhibition can prevent saturation of the spike-generating mechanism of the interneuron. In addition to compensating for changes in input level from a

[4] An alpha function decays to e^{-1} of its peak after a duration of about three times the time-to-peak. Therefore a time-to-peak of 5 ms corresponds roughly to a conductance duration of 15 ms.

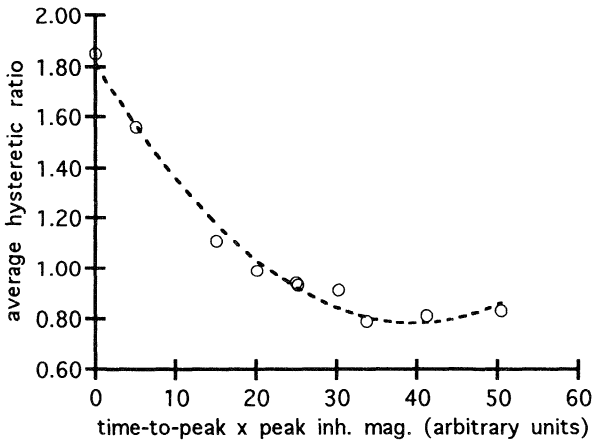

FIG. 15. Hysteretic ratio (see text for definition) averaged over joint angle as a function of the product of synaptic time-to-peak and peak synaptic conductance value of the shunting inhibitory synapses. Dashed line is a 2nd-order polynomial fit to the data.

given set of afferents, this automatic gain control mechanism could also prevent saturation if presynaptic afferents were added during development and could maintain the dynamic range of the interneuron if presynaptic afferents were removed because of damage.

More importantly, we have shown that presynaptic shunting inhibition between sensory afferents can reduce hysteresis in mechanosensory coding. A compartmental model showed that lateral shunting inhibition between proprioceptive afferents compensates for hysteresis in their coding properties despite nonlinearities in their tuning curves and in their synaptic transfer functions. This mechanism works because a uniform increase in afferent firing rate is adaptively offset by a decrease in average postsynaptic conductance, and vice versa. This represents an important new function for lateral inhibition because of the widespread occurrence of hysteresis in sensory systems.

Widely accepted roles of lateral inhibition include the automatic control of input gain (Lyon 1991), sharpening of receptive fields (Ratliff and Hartline 1959; Watson 1992), and the prevention of habituation of sensory afferents (Watson 1992). Lateral inhibition has also been proposed as a data compression mechanism by reducing the redundancy in the input signal. This can be accomplished by reducing the necessary information capacity of each afferent channel through linear prediction (Srinivasan et al. 1982), or by reducing the number of afferent channels through principle component analysis (Földiák 1989). These functions can be thought of as enhancing or optimizing the input signal. Hysteresis reduction is an information processing mechanism that eliminates history dependent features of the input signal so that it represents more accurately the physical state of the system to be controlled. It thus appears that the nervous system may have found a simple solution to the problems most likely created by nonlinear, viscoelastic properties of biological tissues.

How can it be possible that one class of neurons (the spiking interneurons) exhibits reduced hysteresis (Burrows 1985, 1988), whereas another class of neurons (the nonspiking interneurons that drive the motoneurons) does not (Siegler 1981; Siegler and Burrows 1983)? The answer is that there are multiple pathways between proprioceptive afferents and motoneurons. Indeed, Burrows (1987) has shown the existence of parallel pathways in which a single afferent makes direct connections with both motoneurons and spiking local interneurons. Perhaps, monosynaptic or disynaptic pathways via the nonspiking interneurons retain the hysteresis to compensate for muscle catch (Zill and Jepson-Innes 1988), whereas a multisynaptic pathway via certain spiking interneurons reduces the hysteresis to pass on more accurate sensory information to higher centers. Also, by combining the information from hysteretic channels with ones that have eliminated the ambiguity, it should be possible to acquire information not only about the present state of the leg but also its past history of motion.

The results of these simulations suggest a number of testable predictions. First, if hysteresis reduction depends on lateral shunting inhibition between afferents, hysteresis should appear at the spiking interneuron if the presynaptic shunting currents at the afferent terminals are selectively blocked. Second, presynaptic shunting inhibition should occur preferentially between afferents that have similar recruitment thresholds. Burrows and Matheson (1994) already have experimental evidence to partially support this prediction. Third, these results strongly suggest a gradient inhibitory weighting scheme in which shunting presynaptic conductances should be greater onto afferents that are recruited first.[5]

We thank A. Berkowitz, B. Mel, and T. Matheson for critical comments on this manuscript. We also thank H. Zhang for technical assistance with the NEURON simulator.

This work was supported by grants from the National Institutes of Health to G. Laurent and M. Burrows, from the Office of Naval Research to G. Laurent, and by a Searle Scholars Award to G. Laurent. G. Laurent is a National Science Foundation Presidential Faculty Fellow.

Permanent address of M. Burrows: Department of Zoology, University of Cambridge, Downing St., Cambridge CB2 3EJ, England.

Address for reprint requests: N. Hatsopoulos, Department of Neuroscience, Box 1953, Brown University, Providence, RI 02912.

Received 7 June 1994; accepted in final form 21 November 1994.

REFERENCES

ALVAREZ BUYLLA, R. AND RAMIREZ DE ARELLANO, J. Local responses in Pacinian corpuscles. *Am. J. Physiol.* 172: 237–244, 1953.

BROWN, M. C. AND STEIN, R. Quantitative studies on the slowly adapting stretch receptor of the crayfish. *Kybernetik* 3: 175–181, 1966.

BURNS, M. D. Structure and physiology of the locust femoral chordotonal organ. *J. Insect Physiol.* 20: 1319–1339, 1974.

BURROWS, M. The processing of mechanosensory information by spiking local interneurons in the locust. *J. Neurophysiol.* 54: 463–478, 1985.

BURROWS, M. Parallel processing of proprioceptive signals by spiking local interneurons and motor neurons in the locust. *J. Neurosci.* 7: 1064–1080, 1987.

BURROWS, M. Responses of spiking local interneurones in the locust to proprioceptive signals from the femoral chordotonal organ. *J. Comp. Physiol. A Sens. Neural Behav. Physiol.* 164: 207–217, 1988.

BURROWS, M. AND LAURENT, G. Synaptic potentials in the central terminals of locust proprioceptive afferents generated by other afferents from the same sense organ. *J. Neurosci.* 13: 808–819, 1993.

BURROWS, M. AND MATHESON, T. A presynaptic gain control mechanism

[5] This weighting scheme need not necessarily be hard wired but could be adaptively developed with the use of a simple Hebbian-type learning rule. Because the afferent recruited first will on average be more active than the afferent recruited last, larger inhibitory synaptic weights will evolve between a presynaptic neighbor recruited first and a postsynaptic afferent.

among sensory neurons of a locust leg proprioceptor. *J. Neurosci.* 14: 272–282, 1994.

CHAPLAIN, R. A., MICHAELIS, B., AND COENEN, R. Systems analysis of biological receptors. I. Quantitative description of the input-output characteristics of the slowly-adapting stretch receptor on the crayfish. *Kybernetik* 9: 85–95, 1971.

CONNOR, J. A. AND STEVENS, C. F. Voltage-clamp study of a transient outward membrane current in gastropod neural somata. *J. Physiol. Lond.* 213: 21–30, 1971.

FÖLDIÁK, P. Adaptive network for optimal linear feature extraction. In: *International Joint Conference on Neural Networks (Washington 1989).* New York: IEEE, 1989, vol. I, p. 401–405.

FUJITA, Y., ROSENBERG, J., AND SEGUNDO, J. P. Activity of cells in the lateral vestibular nucleus as a function of head position. *J. Physiol. Lond.* 196: 1–18, 1968.

GRIGG, P. AND GREENSPAN, B. J. Response of primate joint afferent neurons to mechanical stimulation of knee joint. *J. Neurophysiol.* 40: 1–8, 1977.

GROSSBERG, S. Contour enhancement, short term memory, and constancies in reverberating neural networks. In: *Studies of Mind and Brain,* edited by S. Grossberg. Dordrecht, Holland: Reidel, 1973, p. 334–378.

GROSSBERG, S. Nonlinear neural networks: principles, mechanisms, and architectures. *Neural Networks* 1: 17–61, 1988.

HAGIWARA, S., KUSANO, K., AND SAITO, N. Membrane changes of Onchidium nerve cell in potassium-rich media. *J. Physiol. Lond.* 155: 470–489, 1961.

HINES, M. A program for simulation of nerve equations with branching geometries. *J. Biomed. Comp.* 24: 55–68, 1989.

HODGKIN, A. L. AND HUXLEY A. F. A quantitative description of membrane current and its application to conduction and excitation in nerve. *J. Physiol. Lond.* 117: 500–544, 1952.

KATZ, B. AND MILEDI, R. The study of synaptic transmission in the absence of nerve impulses. *J. Physiol. Lond.* 189: 535–544, 1967.

KOSTYUKOV, A. I. AND CHERKASSKY, V. L. Movement-dependent aftereffects in the firing of the spindle endings from the de-efferented muscles of the cat hindlimb. *Neuroscience* 46: 989–999, 1992.

LEITCH, B., WATKINS, B. L., AND BURROWS, M. Distribution of acetylcholine-receptors in the central nervous system of adult locusts. *J. Comp. Neurol.* 334: 47–58, 1993.

LENNERSTRAND, G. Position and velocity sensitivity of muscle spindles in the cat. I. Primary and secondary endings deprived of fusimotor activation. *Acta Physiol. Scand.* 73: 281–299, 1968.

LYON, R. F. Automatic gain control in cochlear mechanics. In: *The Mechanics and Biophysics of Hearing,* edited by P. Dallos, C. D. Geisler, J. W. Matthews, M. A. Ruggero, and C. R. Steele. New York: Springer-Verlag, 1991, p. 395–402.

MAJOR, G., LARKMAN, A. U., AND JACK, J. J. B. Constraining non-uniqueness in passive electrical models of cortical pyramidal neurones (Abstract). *J. Physiol. Lond.* 430: 13P, 1990.

MATHESON, T. Responses and locations of neurones in the locust metathoracic femoral chordotonal organ. *J. Comp. Physiol.* 166: 915–927, 1990.

MATHESON, T. Range fractionation in the locust metathoracic femoral chordotonal organ. *J. Comp. Physiol. A Sens. Neural Behav. Physiol.* 170: 509–520, 1992.

MILL, P. J. AND LOWE, D. A. An analysis of the types of sensory unit present in the PD proprioceptor of decapod crustaceans. *J. Exp. Biol.* 56: 509–525, 1972.

MOUNTCASTLE, V. B., POGGIO, G. F., AND WERNER, G. The relation of thalamic cell response to peripheral stimuli varied over an intensity continuum. *J. Neurophysiol.* 26: 807–834, 1963.

PRESS, W. H., FLANNERY, B. P., TEUKOLSKY, S. A., AND VETTERLING, W. T. *Numerical Recipes in C.* Cambridge, UK: Cambridge Univ. Press, 1990.

RALL, W. Distinguishing theoretical synaptic potentials computed for different somadendritic distributions of synaptic inputs. *J. Neurophysiol.* 30: 1138–1168, 1967.

RATLIFF, F. AND HARTLINE, H. K. The responses of Limulus optic nerve fibers to patterns of illumination on the retinal mosaic. *J. Gen. Physiol.* 42: 1241–1255, 1959.

ROGAWSKI, M. A. The A-current: how ubiquitous a feature of excitable cells is it? *Trends Neurosci.* 8: 214–219, 1985.

SATTELLE, D. B. AND BREER, H. Cholinergic nerve terminals in the central nervous system of insects. *J. Neuroendocrinol.* 56: 987–1006, 1990.

SEGUNDO, J. P. AND DIEZ MARTINEZ, O. Dynamic and static hysteresis in crayfish stretch receptors. *Biol. Cybern.* 52: 291–296, 1985.

SHELTON, P. M. J., STEPHEN, R. O., SCOTT, J. J. A., AND TINDALL, A. R. The apodeme complex of the femoral chordotonal organ in the metathoracic leg of the the locust *Schistocerca gregaria. J. Exp. Biol.* 163: 345–358, 1992.

SIEGLER, M. V. S. Postural changes alter synaptic interactions between nonspiking interneurons and motor neurons of the locust. *J. Neurophysiol.* 46: 310–323, 1981.

SIEGLER, M. V. S. AND BURROWS, M. Spiking local interneurons as primary integrators of mechanosensory information in the locust. *J. Neurophysiol.* 50: 1281–1295, 1983.

SMITH, S. J. AND AUGUSTINE, G. J. Calcium ions, active zones and synaptic transmitter release. *Trends Neurosci.* 11: 458–464, 1988.

SPRUSTON, N. AND JOHNSTON, D. Perforated patch-clamp analysis of the passive membrane properties of three classes of hippocampal neurons. *J. Neurophysiol.* 67: 508–529, 1991.

SRINIVASAN, M. V., LAUGHLIN, S. B., AND DUBS, A. Predictive coding: a fresh view of inhibition in the retina. *Proc. R. Soc. Lond. B Biol. Sci.* 216: 427–459, 1982.

WATSON, A. H. D. Presynaptic modulation of sensory afferents in the invertebrate and vertebrate nervous system. *Comp. Biochem. Physiol. A Comp. Physiol.* 103A: 227–239, 1992.

VIDAL, J., JEANNEROD, M., LIFSCHITZ, W., LEVITAN, H., ROSENBERG, J., AND SEGUNDO, J. P. Static and dynamic properties of gravity-sensitive receptors in the cat vestibular system. *Kybernetik* 9: 205–215, 1971.

ZILL, S. N. AND JEPSON-INNES, K. Evolutionary adaptation of a reflex system: sensory hysteresis counters muscle "catch" tension. *J. Comp. Physiol. A Sens. Neural Behav. Physiol.* 164: 43–48, 1988.